THE JOURNAL OF BIOLOGICAL CHEMISTRY
Vol. 278, No. 46, Issue of November 14, pp. 45160–45170, 2003
Printed in U.S.A.

Effect of Clathrin Heavy Chain- and α-Adaptin-specific Small Inhibitory RNAs on Endocytic Accessory Proteins and Receptor Trafficking in HeLa Cells*

Received for publication, July 8, 2003, and in revised form, September 3, 2003
Published, JBC Papers in Press, September 6, 2003, DOI 10.1074/jbc.M307290200

Lars Hinrichsen‡, Jens Harborth§¶, Lars Andrees‡, Klaus Weber§, and Ernst J. Ungewickell‡‖

From the ‡Department of Cell Biology in the Center of Anatomy, Hannover Medical School, D-30623 Hannover, Germany and the §Department of Biochemistry and Cell Biology of the Max-Planck-Institute for Biophysical Chemistry, D-37070 Göttingen, Germany

To assess the contribution of individual endocytic proteins to the assembly of clathrin coated pits, we depleted the clathrin heavy chain and the α-adaptin subunit of AP-2 in HeLa-cells using RNA interference. 48 h after transfection with clathrin heavy chain-specific short interfering RNA both, the heavy and light chains were depleted by more than 80%. Residual clathrin was mainly membrane-associated, and an increase in shallow pits was noted. The membrane-association of adaptors, clathrin assembly lymphoid myeloid leukemia protein (CALM), epsin, dynamin, and Eps15 was only moderately affected by the knockdown and all proteins still displayed a punctate staining distribution. Clathrin depletion inhibited the uptake of transferrin but not that of the epidermal growth factor. However, efficient sorting of the epidermal growth factor into hepatocyte growth factor-regulated tyrosine kinase substrate-positive endosomes was impaired. Depletion of α-adaptin abolished almost completely the plasma membrane association of clathrin. Binding of Eps15 to membranes was strongly and that of CALM moderately reduced. Whereas the uptake of transferrin was efficiently blocked in α-adaptin knockdown cells, the internalization and sorting of the epidermal growth factor was not significantly impaired. Since neither clathrin nor AP-2 is essential for the internalization of EGF, we conclude that it is taken up by an alternative mechanism.

Clathrin-coated vesicles move cell surface receptors to endosomes and return some of them through recycling endosomes back to the plasma membrane (1, 2). Lysosomal enzymes are transported by clathrin coated vesicles from the *trans*-Golgi network (TGN)[1] to the endosomal compartment (1). Moreover, clathrin coats are also involved in the sorting of mono-ubiquitinated proteins into internal vesicles of multivesicular endosomes (MVE) (3). MVE play an essential role in the down-regulation of signaling receptors such as the activated epidermal growth factor receptor (EGFR) (4). Principal structural components of plasma membrane-derived clathrin-coated vesicles are clathrin that consists of three heavy and three light chains and the heterotetrameric adaptor protein AP-2 composed of α, β_2, μ_2, and σ_2 subunits. The structurally related AP-1 adaptor complex is found mainly in the TGN (5). The clathrin coat on MVE does not include any of the conventional adaptor complexes (AP-1, AP-2, or AP-3) (6), but labels positive for the clathrin binding protein Hrs (hepatocyte growth factor-regulated tyrosine kinase substrate) (7).

In addition to adaptors a number of accessory proteins are involved in clathrin coat assembly on the plasma membrane. These include Eps15 and the ENTH domain proteins epsin, CALM, and its neuronal homolog AP180. Epsin and CALM/AP180 can associate through their ENTH domain with the rare membrane lipid phosphatidylinositol 4,5-bisphosphate (PIP_2), which might define the sites of coat assembly (8, 9). Recent evidence suggests that the association of the epsin ENTH domain with the membrane induces an increase in curvature that could support the budding process (10). Epsin also associates directly with the clathrin heavy chain (11, 12) with the α-appendage domain of AP-2 (11–13) and with β_2-appendage domain of AP-2 (14). AP180 associates directly with clathrin and AP-2 (11–18). In general, short protein-protein interaction motifs determine the specificity of the interactions between endocytic proteins with clathrin and adaptors (19). The interaction of the more widely expressed AP180 homolog CALM with AP-2 is not as well documented yet (20). Apart from the ENTH domain, the polypeptide chain of both, epsin and AP180, are largely disordered (21). This property might allow the efficient recruitment of AP-2 and clathrin to sites of coat assembly. In fact it was recently demonstrated that the proteins AP180, AP-2, and clathrin are sufficient to induce clathrin-coated buds on PIP_2-containing monolayers (8). The endocytic accessory protein Eps15 interacts with the appendage domain of α-adaptin (22) but not with clathrin (23). By immunoelectron microscopy it was detected on the rim of plasma membrane clathrin-coated pits (24) and on the limiting membrane of early endosomes (25) where it is likely to associate with Hrs (26, 27). The function of Eps15 on endosomes is not yet fully understood but transfection experiments with dominant negative mutant Eps15 have indicated that it is essential for the recruitment of AP-2 to the plasma membrane (28).

There are numerous other endocytic proteins not mentioned so far that are either involved in the recruitment of specific

* This work was supported by the German Research Foundation and the Fond der Chemischen Industrie. The costs of publication of this article were defrayed in part by the payment of page charges. This article must therefore be hereby marked "*advertisement*" in accordance with 18 U.S.C. Section 1734 solely to indicate this fact.

¶ Current address: Alnylam Pharmaceuticals, 790 Memorial Dr., Suite 202, Cambridge, MA 02139.

‖ To whom correspondence should be addressed. Fax: 49-511-532-3903; E-mail: ungewickell.ernst@mh-hannover.de.

[1] The abbreviations used are: TGN, *trans*-Golgi network; BSA, bovine serum albumin; CALM, clathrin assembly lymphoid myeloid leukemia protein; EEA1, early endosomal antigen 1; EGF, epidermal growth factor; EGFR, epidermal growth factor receptor; EH domain, Eps15 homology domain; ENTH, epsin N-terminal homology domain; Hrs, hepatocyte growth factor-regulated tyrosine kinase substrate; MVE, multivesicular endosomes; PBS, phosphate-buffered saline; TBS, Tris-buffered saline; PIP_2, phosphatidylinositol 4,5-bisphosphate; RNAi, RNA interference; siRNA, short interfering RNA; HC, heavy chain; LC, light chain.

cargo, *e.g.* β-arrestin and Dab2 (29–32), into coated pits or they function like amphiphysin and dynamin at downstream stages of the budding and fission process (33–36). Upon the release of coated vesicles into the cytosol, the clathrin coat is removed by the combined action of auxilins, hsc70 and synaptojanin (37–42). Other endocytic accessory proteins such as HIP1/HIP1R and intersectin are linking clathrin-mediated endocytosis to the actin-based cytoskeleton (reviewed in Ref. 43).

The function of novel putative endocytic proteins discovered in the past by homology searches, proteomic approaches, yeast two-hybrid screens or other means was mostly confirmed by their inhibitory effects on receptor internalization when overexpressed as dominant negative variants. While this clearly indicates an involvement of the overexpressed protein in endocytosis, it often tells little about the stage in the endocytic process where a particular protein is needed. Clathrin coat formation seems to be governed by a complex web of reversible protein-protein interactions that engage under tight temporal and spatial regulation. Overexpression of almost any component of the endocytic machinery often results in its complete collapse due to the unregulated sequestration of one or more interaction partners. Therefore, alternative approaches have been developed that aim at the elimination of select components or of their genes. Among the most powerful methodologies for reducing the cellular concentration of proteins is RNA interference (RNAi). Recently this technique was adopted to mammalian cells where the transfection of 21-nucleotide RNA duplexes with two nucleotide 3′ overhang resulted in the specific degradation of cognate mRNA and thus in the depletion of the encoded protein (44).

Here we employed RNAi in HeLa cells to reduce the cellular concentration of the clathrin heavy chain and that of the AP-2 α-adaptin subunit. The transfected cells were examined by immunofluorescence, Western blotting, cell fractionation, electron microscopy, and functional endocytosis assays. Our results indicated that both proteins were efficiently depleted from the transfected cells within 48 h. The knockdown of clathrin heavy chain was paralleled by the disappearance of clathrin light chains. Residual clathrin on the plasma membrane was mainly found in shallow coated pits. The membrane association of the endocytic proteins AP-2, CALM, and epsin was only marginally affected. Transferrin uptake was strongly inhibited in the knockdown cells, but the uptake of EGF appeared to be normal. However, intracellular trafficking of the EGF was impaired. Moreover, the intracellular distribution of the early endosomal marker EEA1, of Hrs, and that of the large mannose 6-phosphate receptor was altered upon clathrin depletion. α-Adaptin depletion had a strong effect on the membrane association of both clathrin and Eps15. It also inhibited transferrin uptake but had no effect on EGF internalization.

EXPERIMENTAL PROCEDURES

Antibodies and Reagents—Mouse monoclonal antibodies used for immunofluorescence were as follows: X22, anti-clathrin heavy chain (45); AP.6, anti-α-adaptin (46); monoclonal antibody 100/3, anti-γ-adaptin, (47); anti-EEA1 (BD Biosciences, catalog number 610456).

Mouse monoclonal antibodies used for Western blotting were as follows: monoclonal antibody 100/1 anti-β-adaptin (47), anti-clathrin heavy chain (BD Biosciences, catalog number 610500), anti-α-adaptin (Santa Cruz Biotechnology, catalog number sc-17771, Santa Cruz, CA), and anti-μ_2 (AP-50 from BD Biosciences).

Rabbit polyconal antibodies for immunofluorescence and Western blotting were as follows: affinity-purified R461 directed against clathrin light chains (47). Antisera directed against CALM were raised against the peptide CRPPNPFGPVPGAAQIQFM, and antisera directed against Eps15 were raised against the peptide CQEDLELAIALSKSEISEA. To generate an antibody against epsin, the peptide CEERIRRGDDLRLQMA was used as antigen. Peptide synthesis and custom immunizations were performed by BioScience (Göttingen, Germany). Actin was detected on Western blots by the affinity-purified serum R442-6 raised against bovine actin in our laboratory. For most applications the polyclonal sera were affinity-purified using the respective peptides attached to Sulfo-link resin (Pierce). The purified antibodies were eluted with 0.1 M glycine, pH 2.5. The polyclonal rabbit antibody against the cation-independent mannose 6-phosphate receptor was obtained from B. Hoflack (Max-Planck-Institut für Zellbiologie und Genetik, Dresden, Germany). A polyclonal rabbit antibody against EEA1 was from M. Zerial (Max-Planck-Institut für Zellbiologie und Genetik, Dresden, Germany) and H. Stenmark (Oslo, Norway) provided the polyclonal rabbit serum against Hrs. A second polyclonal rabbit antibody against epsin that was used for staining epsin in cells was obtained from L. Traub (Pittsburgh, PA) (17). Fluorescein isothiocyanate and rhodamine-labeled anti-mouse or anti-rabbit antibodies were from Molecular Probes (Leiden, The Netherlands). Secondary horseradish peroxidase-conjugated anti-mouse or anti-rabbit antibodies were from ICN (Aurora, OH). Biotin-labeled transferrin (Molecular Probes) was detected by NeutrAvidin coupled to horseradish peroxidase (Molecular Probes). Texas Red-labeled EGF and Texas Red-labeled transferrin were from Molecular Probes. ^{125}I-labeled EGF (6.25 MBq/μg) was obtained from New England Nuclear/PerkinElmer Life Sciences (Zaventem, Belgium).

siRNA—The clathrin heavy chain siRNAs (AACCUGCGGUCUGGAGUCAAC, HC oligo I, and AAUGGAUCUCUUUGAAUACGG, HC oligo II) was obtained from Dharmacon (Lafayette, CO). The α-adaptin siRNA (GAGCAUGUGCACGCUGGCCAGCU, α-oligo I) was purchased from Proligo (Hamburg, Germany), and a second α-adaptin siRNA (AAGAGGUGUGGUACCGAGUCA (α-oligo II)) was from Dharmacon. Firefly (*Photinus pyralis*) luciferase siRNA (AACGTTACCGCGGAATACTTCGA) was obtained from Dharmacon. Selected sequences were submitted to BLAST searches against the human genome sequence to ensure that only the desired mRNA was targeted. siRNA duplex formation was performed as described elsewhere (44).

Cell Culture and Transfection—HeLa SS6 cells were grown at 37 °C and 5% CO_2 in Dulbecco's modified Eagle's medium (Invitrogen, Karlsruhe, Germany) supplemented with 10% fetal calf serum (Seromed, Berlin, Germany), 1 mM sodium pyruvate (Sigma, Taufkirchen, Germany), 100 units/ml penicillin, and 100 μg/ml streptomycin (Invitrogen). Cells were regularly passaged to maintain exponential growth. 24 h before transfection with siRNA the cells were trypsin-digested and resuspended at a density of $0.5–0.8 \times 10^5$ cells/ml in fresh medium containing 10% fetal calf serum but no pyruvate or antibiotics. For most experiments the cells were seeded in 24-well plates (Nunc, Wiesbaden, Germany). Oligofectamine (Invitrogen) was used for the delivery of siRNAs into HeLa cells following the procedure of Harborth *et al*. (48). For 3×10^4 cells 60 pmol of RNA duplex were used. Control cells were transfected with firefly luciferase siRNA. For some experiments the luciferase siRNA was omitted, because we noted that the transfection reagent was the sole cause for any transient cellular stress. The final volume of the transfection mixture was 600 μl per well. Cells were assayed 48 h after transfection unless indicated otherwise in the legends to the figures. The extent of gene silencing was assessed by Western blotting of cell lysates. To control for any differences in cell numbers the signal of the silenced protein was related to that of actin. Alternatively, in some experiments the signal originating from the targeted protein was related to total cellular protein as determined by BCA-200 protein assay (Pierce). Data shown represent averages of three independent transfection experiments performed in parallel.

Western Blotting—For Western blotting siRNA-treated cells were trypsin-digested in 24-well plates at 37 °C until the cells detached. The protease was stopped with cold medium containing 10% fetal calf serum. Subsequently the cells were washed with PBS and then solubilized in hot SDS sample buffer. Proteins were separated by SDS-PAGE using 9–19% gradient gels (49) and then electroblotted onto Protran nitrocellulose transfer membrane (Schleicher & Schüll, Dassel, Germany). Horseradish-conjugated secondary antibodies were visualized using the chemiluminescence reagent detection system from PerkinElmer Life Sciences (Zaventem, Belgium). In case of reprobing the membrane with different primary antibodies, the membranes were stripped for 30 min at 50 °C in a buffer containing 62.5 mM Tris-HCl, 100 mM β-mercaptoethanol, 2% SDS, pH 6.7.

Immunofluorescence Microscopy—For immunofluorescence cells were grown and transfected on glass cover slips which were placed in 24-well plates. For some experiments cells transfected with clathrin or α-adaptin siRNA were trypsin-digested after 24 h and mixed with approximately the same number of control cells and then replated on glass cover slips. This allowed viewing and photographing control and knockdown cells next to each other within the same field. 48 h after

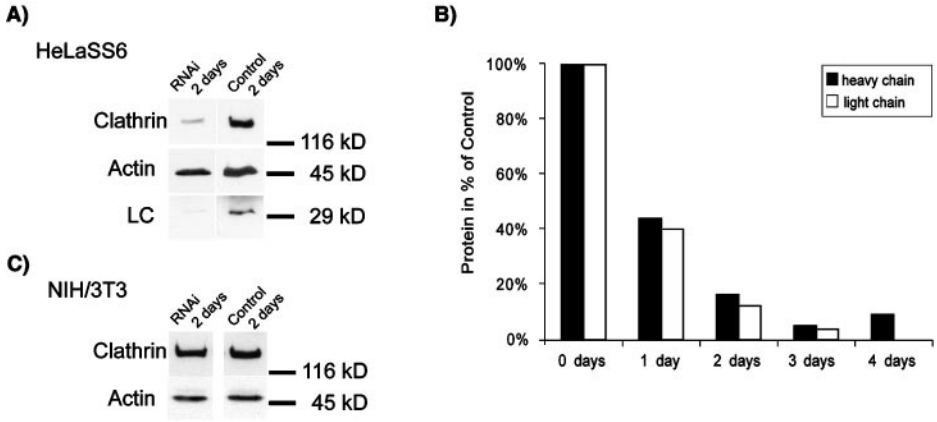

FIG. 1. **Clathrin HC depletion in HeLa cells by transfection with siRNA.** *A*, Western blot analysis of lysates from clathrin siRNA-transfected and mock-transfected cells stained for clathrin heavy chain, light chain, and actin. Lysates were prepared 48 h after transfection. *B*, time course of the heavy chain knockdown. Band intensities of clathrin heavy and light chain were quantified by densitometry and divided by the actin signal to account for differences in sample loadings. Mock-transfected cells were set as 100%. The data show that the clathrin heavy chain is effectively depleted already 48 h post-transfection. Note that the reduction of the heavy chain is paralleled by the disappearance of the clathrin light chain. The data are averages of two independent experiments. *C*, Western blot analysis of lysates from clathrin siRNA-transfected and mock-transfected NIH 3T3 mouse fibroblasts cells stained for clathrin heavy chain and actin. Note that the human-specific RNA duplex had no effect on the expression of mouse clathrin heavy chain.

transfection they were fixed for 10 min at room temperature in 4% formaldehyde solution prepared by dissolving paraformaldehyde in 2.7 mM KCl, 1.9 mM KH_2PO_4, 8.2 mM Na_2PO_4, 137 mM NaCl, pH 7.4 (PBS). The fixative was either used freshly or stored in aliquots at −20 °C. After fixation the cells were washed three times with 20 mM Tris-HCl, 140 mM NaCl, pH 7.6 (TBS) and then permeabilized with 0.1% Triton X-100 in TBS for 5 min. After permeabilization the cells were washed in PBS and then incubated with the primary antibody for 1 h at 37 °C. Primary antibodies were diluted with PBS containing 3% BSA. The cover slips were thoroughly washed between the incubations with primary and secondary antibodies. The secondary antibody was also diluted with 3% BSA in PBS and the incubation time was 1 h at 37 °C. Nuclei were stained with Hoechst 33342 (Molecular Probes) (1 μM in 3% BSA/PBS) for 10 min on ice. Finally the cells were embedded in Prolong Antifade (Molecular Probes). Labeled cells were viewed with a Nikon Eclipse E800 microscope equipped with Epi-fluorescence attachment (Nikon, Tokyo, Japan). Images were recorded with a CCD camera (Princeton Instruments, Trenton, NJ) using IPLab software (Scanalytics, Inc., Fairfax, VA). Final figures were arranged with Adobe Photoshop version 5.0 and Illustrator Version 8.0 (Adobe, San Jose, CA).

EGF and Transferrin Uptake Assays—48 h after transfection the cells were serum starved for 30 min with medium containing 0.1% BSA at 37 °C. For immunofluorescence studies 20 μl of Texas Red-labeled EGF (10 ng/ml in culture medium supplemented with 0.1% BSA) or 20 μl of Texas Red-labeled transferrin (5 μg/ml in culture medium supplemented with 0.1% BSA), respectively, were applied to cells grown on glass coverslips and incubated for 1 h on ice. For quantitative uptake assays, 120 μl of ^{125}I-labeled EGF (10 ng/ml) or biotin-labeled transferrin (250 ng/ml), respectively, were used per well of a 24-well plate that contained ~10^5 cells. Unbound ligand was removed by quick washes with prewarmed serum free medium, and bound ligand was allowed to be internalized upon incubation in 0.1% BSA-containing medium for varies lengths of time at 37 °C. For immunofluorescence studies the cells were processed as described above. For quantitative uptake experiments unbound ligand (^{125}I-labeled EGF or biotin-labeled transferrin) was removed by a 2.5-min incubation in 0.5 M NaCl, 0.2 M sodium acetate buffer, pH 4.5, followed by a wash cycle with the same solution (50). Cells incubated with radioactively labeled EGF were then lysed in hot 0.1 M Tris-HCl, pH 8, supplemented with 1% SDS and counted in a γ-counter (Berthold BF 2111, Wildbad, Germany). Internalized biotinylated transferrin was quantitated by Western blotting using NeutrAvidin conjugated to horseradish peroxidase. Signals were detected by chemiluminescence.

Cell Fractionation—siRNA transfected HeLa cells were grown in 2-ml dishes (Nunc) for 48 h and then washed first with PBS and then with ice-cold lyses buffer (100 mM sodium phosphate, 50 mM NaCl, 1 mM $MgCl_2$, 1 mM EGTA, pH 7.4) containing Complete Mini-protease inhibitor mixture (Roche, Grenzach, Germany). The cells were freeze-thawed twice in 0.3 ml of lyses buffer and collected by scraping. The suspension was centrifuged for 45 min at 90,000 × *g* in a Beckman Optima TL bench top ultracentrifuge (Beckman Coulter Inc., Fullerton, CA) at 4 °C. Both supernatant and pellet fractions were denatured in SDS-sample buffer and subjected to SDS-PAGE and Western blotting.

Electron Microscopy—siRNA transfected and control cells grown in 24-well plates were washed twice with PBS and then fixed for 30 min with 2.5% glutaraldehyde in 0.1 M cacodylate buffer, pH 7.3. Subsequently the cells were washed for 10 min with 0.5 ml of cacodylate buffer, incubated for 1 h in a solution containing 1% osmium tetroxide, and then dehydrated in an ascending series of 25, 50, 75, and 100% ethanol. The cells were detached from the surface of the well with propylenoxide, transferred to a reaction tube, pelleted, supplemented with a 1:1 mixture of Epon and propylenoxide, and incubated for 30 min at 40 °C. Next they were transferred into a solution of 25% propylenoxide and 75% Epon and incubated for 90 min at 40 °C. This was followed by an incubation for 45 min at 40 °C in pure Epon. The Epon was once more replaced and then allowed to polymerize for 20 h at 40 °C and followed by 40 h at 60 °C. 50–70-nm sections were cut using an Ultrotom III Ultramicrotom (LKB, Bromma, Sweden). Sections were placed on copper grids and contrasted with lead citrate and 10% uranyl acetate. The sections were viewed with a Zeiss EM902 electron microscope (Zeiss, Oberkochen, Germany).

RESULTS

Effect of Clathrin Heavy Chain Depletion on Associated Proteins—To inhibit the expression of the clathrin heavy chain, we selected an siRNA duplex that targeted the segment 3311–3333 of the heavy chain open reading frame. Control cells were transfected with a control siRNA (luciferase) or with the transfection reagent alone, because the presence of the luciferase siRNA did not affect the cells. To quantitate the reduction in clathrin heavy chain expression the transfected cells were lysed in SDS-sample buffer and analyzed by immunoblotting with antibodies directed against the clathrin heavy chain, clathrin light chain and actin as a control, respectively (Fig. 1*A*). This analysis was performed with aliquots taken before the transfection (day 0) and then daily until day 4. On the second day after transfection both, the signals from the clathrin heavy and light chains were strongly reduced, whereas the actin signals had changed only slightly. Quantification of the data by densitometry and normalization relative to the actin signals showed that the cellular concentration of the clathrin heavy chain had dropped to 16% on day 2 compared with control cells (Fig. 1*B*). The lowest level of about 5% was reached on day 3. Day 4 showed a slight recovery of the heavy chain signal, which is probably due to the growth of poorly or non-transfected cells. The decrease in cellular heavy chain concentration is mirrored by that of the light chains as shown with a polyclonal antiserum which recognizes preferentially the

smaller of the two light chains (Fig. 1, *A* and *B*). This observation suggests that light chains are not stable unless complexed with heavy chains. We also noted that the heavy chain knockdown affected the viability of cells when only 0.2×10^5 cells/cm^2 were seeded. Usually after 4 days the majority of the cells had died. When the cell number was doubled or tripled, the cells survived, but 48 h after transfection their number still reached only 40% of those that were transfected with luciferase siRNA. The cells did not undergo apoptosis, since neither *in situ* end labeling using terminal deoxynucleotidyltransferase and fluorescein deoxy-UTP or staining for the presence of the caspase cleavage product of cytokeratin 18 (51) gave any indication of increased apoptosis in knockdown cells (data not shown). Thus, the lower cell number after inhibition of heavy chain expression is likely the result of impaired proliferation. Usually we analyzed cells seeded at high density 2 days after transfection. The time course of the reduction of the clathrin heavy chain indicates a half-life of 18–20 h for clathrin in transfected HeLa cells. This is in agreement with the half-life of clathrin in DT40 lymphocytes upon controlled shut down of clathrin heavy chain expression using a tetracyclin-regulatable expression system (52). However, in another report a half-life of 50 h was determined for clathrin in a B cell line (53). We do not yet understand the reasons for this apparent discrepancy.

Gene silencing by RNAi is known to be highly specific (54). Even small changes between target and siRNA sequence render the latter ineffective. The clathrin siRNA (HC oligo I) that was used to silence the clathrin heavy chain gene in human HeLa cells targets a region in the human clathrin mRNA, which differs in several positions from the mouse heavy chain sequence. Therefore, mouse 3T3 fibroblasts served as an excellent control for our selected clathrin siRNA, since it failed to silence the expression of the mouse clathrin heavy chain (Fig. 1*C*).

Immunofluorescence clearly showed that the typical dot-like staining pattern of clathrin heavy and light chains was reduced in the transfected cells as expected from the immunoblotting results (Fig. 2). For the analysis of most of our immunofluorescence experiments clathrin siRNA-treated and control cells were trypsin-digested 24 h after transfection, then mixed and re-plated. This procedure allowed the microscopic observation of control and transfected cells within the same field. When clathrin heavy chain knockdown cells were stained with the affinity-purified polyclonal anti-light chain serum, we noted that this antibody was generally slightly more sensitive than the monoclonal antibody X22, which is directed against the clathrin heavy chain. This is probably due to the recognition of more than one epitope and/or a better accessibility of the light chain epitopes by the polyclonal serum rather than to a heavy chain-independent association of light chains with membranes (Fig. 2, *A* and *A′*). Despite this minor difference the anti-light chain serum served as a faithful indicator for the clathrin heavy chain knockdown in HeLa cells. Close inspection of the transfected cells revealed that after 2 days the clathrin signal was generally weak, but it did not disappear completely. Especially in the perinuclear area where the density of clathrin coated structures is usually the highest, some residual staining was often still evident (Fig. 2, *A* and *A′*). We could duplicate this result with a different RNA duplex that targeted the segment 564–582 encoding residues of the clathrin N-terminal domain (Fig. 2, *B* and *B′*).

Next we determined whether the localization of the adaptor complexes AP-2 and AP-1 or other endocytic accessory proteins were affected by silencing the expression of the clathrin heavy chain gene. Antibodies to AP-2 show a punctate staining pattern originating mostly from coated structures on the plasma membrane. This pattern remained unchanged after clathrin heavy chain depletion (Fig. 2, *C* and *C′*). If at all, the intensity of the AP-2 dots were only slightly diminished and accompanied by a weak diffuse cytosolic staining. In control cells the AP-1 adaptor localizes mostly to the perinuclear area, but it is also present at peripheral vesicular structures (1, 55). After clathrin depletion AP-1-positive structures seemed to be more tightly confined to the perinuclear area (Fig. 2, *D* and *D′*).

A number of endocytic accessory proteins have been postulated to coordinate the assembly of clathrin-coated pits on the plasma membrane. Among those are the proteins CALM and its neuronal homolog AP180, epsin, and Eps15. CALM/AP180 and epsin can associate directly with clathrin and AP-2. Through their respective ENTH domains they can also directly interact with the rare phospholipid PIP_2 (8, 56, 57). To determine whether the association of accessory proteins with the plasma membrane is altered upon clathrin heavy chain knockdown, we analyzed their cellular distribution in HeLa cells. In control cells CALM colocalized perfectly with plasma membrane clathrin coated pits as described previously (20) (Fig. 2, *E* and *E′*). Upon clathrin knockdown the distribution of CALM was not significantly altered (Fig. 2, *E* and *E′*). The next protein we looked at was Eps15. Our immunofluorescence results were consistent with its association with AP-2. Surprisingly when the clathrin heavy chain was knocked down, the staining intensity of Eps15 increased significantly (Fig. 2, *F* and *F′*). This could be explained either by an increased accessibility of Eps15 for the primary antibody or by an increased membrane association in the absence of clathrin. In contrast to the results obtained for Eps15, the cellular distribution and staining intensity of epsin was not significantly affected by the clathrin knockdown (Fig. 2, *G* and *G′*). In conclusion our data show that the endocytic accessory proteins CALM, epsin, and Eps15 appear not to depend on clathrin for their stable association with the plasma membrane.

Clathrin sorts the mannose 6-phosphate receptor from TGN to the endosomal compartment and probably back from there to the TGN (58). Upon clathrin depletion the receptor appeared more concentrated within the perinuclear area (Fig. 2, *H* and *H′*). Clathrin is also present on endosomal membranes where it functions in receptor sorting (5). The early endosomal marker EEA1 was used to test by immunofluorescence whether endosomes were also affected by the clathrin knockdown. EEA1-positive structures are usually dispersed throughout the cytoplasm in control cells. However, upon silencing of clathrin expression the endosomes clustered within the perinuclear area (Fig. 2, *I* and *I′*). A similar observation was made by Bennett *et al.* (60) who demonstrated that overexpression of clathrin hubs induced perinuclear aggregation of endosomes. Recently it was shown that the hepatocyte growth factor-regulated tyrosine kinase substrate (Hrs) recruits clathrin to early endosomes (61). Its cellular distribution overlaps with that of EEA1 in baby hamster kidney cells (62). We made similar observations in HeLa cells. Interestingly, after clathrin knockdown Hrs was also found on large perinuclear structures (Fig. 2, *J* and *J′*) that contained EEA1 (Fig. 2, *K* and *K′*).

Biochemical Analysis of Clathrin Knockdown Cells—To quantitatively examine the effect of clathrin heavy chain depletion on the membrane association of residual clathrin, adaptors, and endocytic accessory proteins, homogenates from control and clathrin knockdown cells were prepared and fractionated by ultracentrifugation into a membrane and cytosolic pool. We employed a homogenization buffer that ensured the stability of the coat of coated vesicles (Fig. 3*A*), but unlike coated vesicle isolation buffer (63), it also prevented spontaneous self-assembly of cytosolic coat components (data not

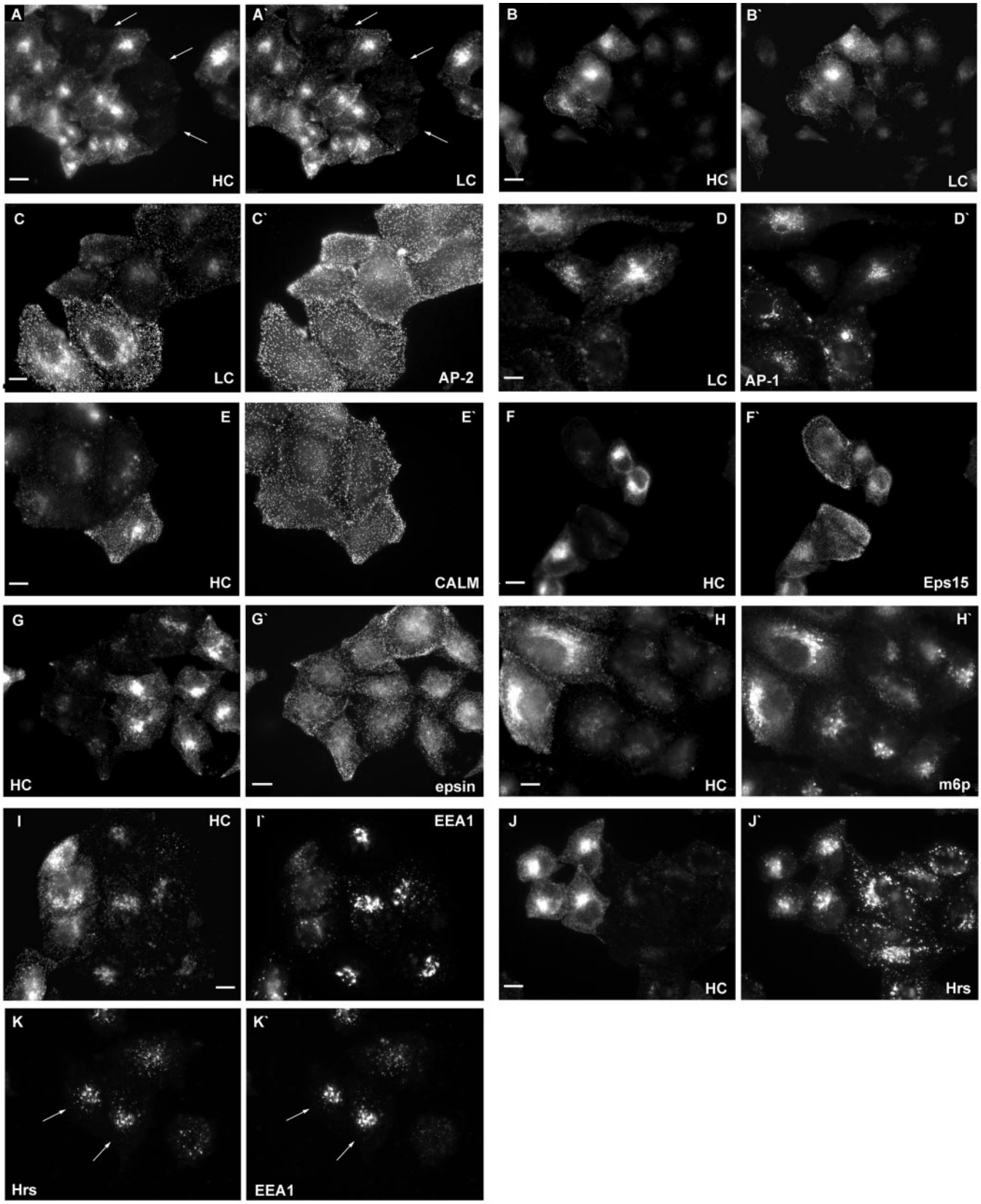

FIG. 2. **Effect of clathrin HC depletion on clathrin-associated proteins and cargo.** 24 h after transfection HeLa cells treated with clathrin HC-specific siRNAs and mock-transfected cells were trypsinized, mixed, and grown for another 24 h on coverslips. This made it possible to view knockdown and control cells within the same field. The cultures were double stained for: clathrin HC with X22 and light chains (LC) with R461 after transfection with HC-oligo I (*A* and *A′*) (the *arrows* point at cells with strongly reduced clathrin staining), clathrin HC with X22 and LC with R461 after transfection with HC oligo II (*B* and *B′*), clathrin LC and the α-adaptin subunit of AP-2 with AP.6 (*C* and *C′*), LC and the γ-adaptin subunit of AP-1 with 20D6 (*D* and *D′*), HC and CALM (*E* and *E′*), HC and Eps15 (*F* and *F′*), HC and epsin (*G* and *G′*), HC and mannose 6-phosphate receptor (*m6p*) (*H* and *H′*), HC and EEA1 (*I* and *I′*), HC and Hrs (*J* and *J′*), Hrs and EEA1 (*K* and *K′*) (the *arrows* point at cells that are likely to be depleted in clathrin). Cells in *C* to *K* were transfected with HC oligo I. The *bar* corresponds to 10 μm.

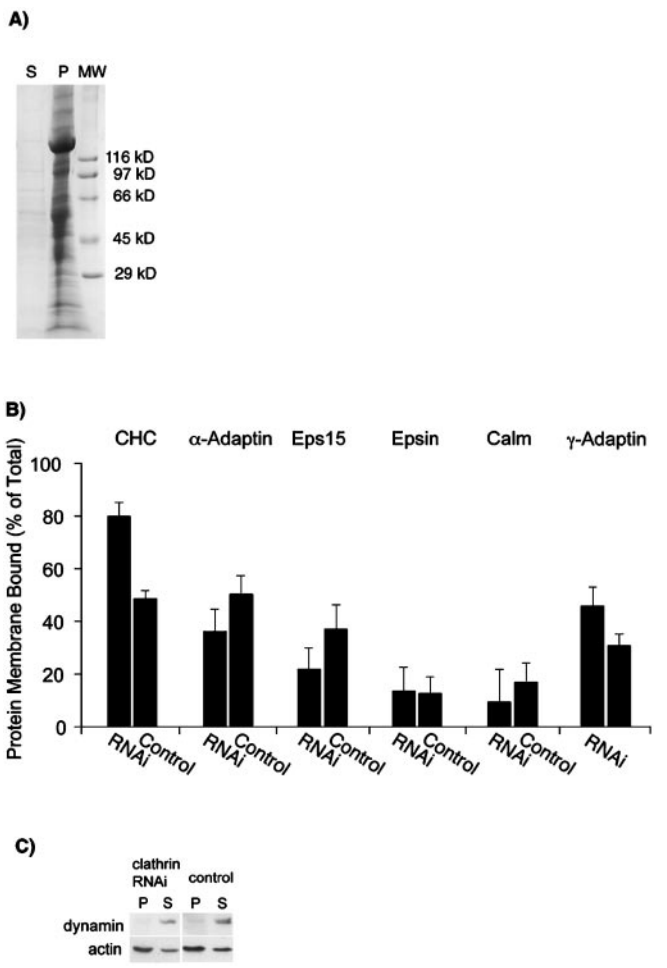

FIG. 3. **Effect of clathrin depletion on the membrane association of coat proteins.** *A*, stability of coated vesicles in lyses buffer. Clathrin-coated vesicles were incubated for 15 min on ice with lyses buffer and pelleted afterward by ultracentrifugation. Supernatant (*S*) and pellet (*P*) were analyzed by SDS-PAGE. Note that lyses buffer does not solubilize the coat proteins from the membrane. *B*, membrane association of coat proteins and endocytic accessory proteins upon clathrin depletion. Cells were scraped off the surface from the tissue culture plates in lyses buffer and fractionated by ultracentrifugation into membrane and cytosol fraction. Both were analyzed by Western blotting. *C*, effect of clathrin depletion on cellular dynamin concentration. The *error bars* show the deviation within data from three independent samples that were analyzed in duplicates by Western blotting.

shown). The analysis of both pools by SDS-PAGE and Western blotting showed that the membrane association of residual clathrin was increased from 49 to 80% (Fig. 3, *B* and *C*). Likewise the membrane-bound form of the Golgi-adaptor AP-1 was slightly increased after clathrin knockdown. In contrast the membrane-bound fraction of AP-2, Eps15, and CALM, respectively, was slightly reduced, whereas that of epsin and dynamin remained unchanged (Fig. 3*B*). We did not observe any significant increases or decreases of the total cellular concentration of any of the aforementioned adaptor or accessory proteins upon depletion of the clathrin heavy chain expression. This was also true for dynamin, which is inconsistent with the recent report (64) of a 10-fold increase in dynamin levels upon a 10% reduction of clathrin expression by antisense RNA (Fig. 3*C*).

Ultrastructural Analysis of Clathrin Knockdown Cells—Ultrathin sections of control and clathrin knockdown cells, fixed 48 h after transfection, were viewed by electron microscopy. We generally noticed a reduction in peripheral clathrin-coated membranes profiles by at least 60%. The data were obtained

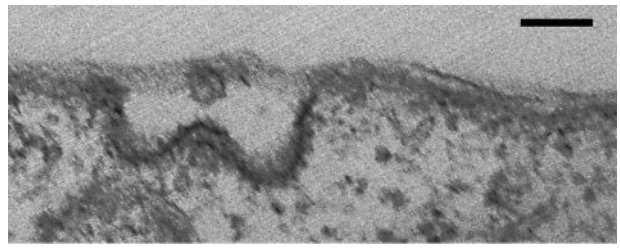

FIG. 4. **Electron micrograph of shallow clathrin-coated after clathrin depletion.** These structures were frequently seen 48 h after transfection with clathrin siRNA but rarely in control cells. *Bar*: 100 nm.

from three independent experiments and based on the analysis of at least 10 complete cell profiles taken from each experiment. It was also observed that the ratio of shallow coated pits (defined by a greater width than depth) to deep invaginated ones changed from 0.6 in controls to 2.3 in clathrin knockdown cells. This suggests that bud formation might be impaired upon clathrin depletion (Fig. 4). The frequent occurrence of adjacent shallow coated dimples in knockdown cells might be a related phenomenon (Fig. 4).

Effects of α-Adaptin Depletion on Clathrin and Endocytic Accessory Proteins—The AP-2 adaptor is considered to be a major organizer of clathrin coats on the plasma membrane where it interacts with cargo, lipid, accessory proteins, and clathrin. However, endocytic accessory proteins such as AP180/CALM are also capable of recruiting clathrin to liposomes and lipid monolayers (8). It was therefore of interest to knockdown the α-adaptin subunit of AP-2. The target of the siRNA was the cDNA segment 1053–1075, which corresponds to codons 351–356 of human αc-adaptin. The α-adaptin-specific siRNA efficiently reduced the expression of α-adaptin by about 95% within 24 h (Fig. 5, *A* and *B*). This result suggested that the α-adaptin has a very high turnover rate. After 48 h depletion of α-adaptin resulted in a 40% decrease in cell numbers compared with the observed 60% decrease upon clathrin depletion indicating that HeLa cells adjust better to the loss of α-adaptin than to that of the clathrin heavy chain. The knockdown of the α-adaptin subunit of AP-2 affected also the stability of the μ_2- and the β-type subunits (Fig. 5*A*). μ_2 was reduced to about 30% and the β-type subunits to ~80%. The difference in the extend of the reduction between the β-type subunits and μ_2 is readily explained by the fact that the monoclonal antibody 100/1 used for Western blotting recognizes both the β_2 subunit, which is part of AP-2, and the highly related β_1, which is a component of the AP-1 adaptor complex (47). Only the β_2 subunit is expected to become instable in the absence of the α subunit. Inhibition of α-adaptin expression was also seen in mouse fibroblasts with α-oligo I siRNA (Fig. 5*C*). This was expected, since α-oligo I targets a region that is conserved between mouse and man.

Immunofluorescence analysis performed after 24 h showed that the α-adaptin signal was strongly reduced in transfected cells. This was paralleled by a strong reduction of the peripheral clathrin light chain signal (Fig. 6, *A* and *A′*). A second siRNA duplex targetting the nucleotide sequence 1498–1518 (codons 460–466) had similar effects on the expression of α-adaptin (*inset* to Fig. 6*A*). By electron microscopy we could confirm an almost complete absence of peripheral clathrin-coated membrane profiles (data not shown). These results suggest that the AP-2 adaptor is essential for the stable recruitment of clathrin to the plasma membrane. It was also of interest to examine the effect of α-adaptin depletion on Eps15, because in previous reports it was suggested that Eps15 is constitutively associated with AP-2 and required for the recruitment of AP-2 to the plasma membrane (23, 65). By immu-

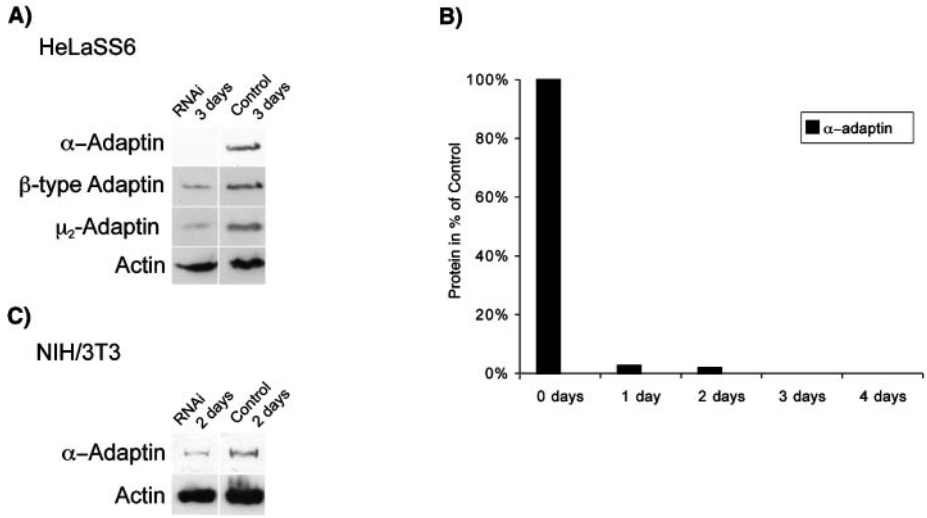

FIG. 5. **siRNA-induced α-adaptin depletion in HeLa cells.** *A*, Western blot of lysates from knockdown-transfected and mock-transfected cells stained for α-adaptin and actin 48 h after transfection. *B*, normalized time course of the depletion. Note that in contrast to clathrin (Fig. 1) α-adaptin is almost completely eliminated from the transfected cells within 24 h. *C*, Western blot analysis of lysates from α-adaptin siRNA-transfected and mock-transfected NIH 3T3 mouse fibroblasts cells stained for α-adaptin and actin. Note that α-oligo I reduced also the expression of mouse α-adaptin.

nofluorescence we noted in α-adaptin siRNA-treated cells that the association of Eps15 with the plasma membrane appeared to be significantly reduced but less than that of α-adaptin (Fig. 6, *B* and *B′*). The intensities of CALM (Fig. 6, *C* and *C′*) and epsin (Fig. 6, *D* and *D′*) were slightly reduced in the α-adaptin knockdown cells. Cell fractionation showed that the α-adaptin depletion decreased the amount of membrane-associated clathrin by about 30%, that of Eps15 by 77%, and that of CALM by 46% (Fig. 7). The membrane-associated fraction of residual α-adaptin increased by about 24% whereas that of epsin remained unchanged (Fig. 7).

Taken together, our results show that for the organization of clathrin in coated plasma membrane patches the α-adaptin subunit of AP-2 is of major importance. Moreover it also stabilizes the plasma membrane association of Eps15.

Differential Effects of Clathrin and α-Adaptin Knockdowns on Receptor-mediated Endocytosis and Receptor Sorting—The effects of clathrin and α-adaptin knockdowns on the endocytosis of transferrin and EGF were investigated by immunofluorescence and quantitative uptake assays. The clathrin knockdown strongly inhibited the uptake of fluorescently labeled transferrin (Fig. 8*A*). Similarly, treating cells with α-adaptin siRNA efficiently reduced the uptake of transferrin (Fig. 8, *C* and *C′*). These results were confirmed by quantitative uptake assays utilizing biotinylated transferrin (Fig. 9, *A* and *B*). Somewhat different and more complex results were obtained for the uptake of fluorescently labeled EGF. In control cells EGF accumulates within 10 min in EEA1 and Hrs-positive structures that probably correspond to multivesicular endosomes (3). Upon knocking down clathrin the staining pattern of EGF was different. Instead of concentrating in endosomal structures the EGF was present in numerous small vesicular structures of low fluorescent intensity (Fig. 8, *B* and *B′* and *inset*). To confirm that EGF was actually taken up by the cells, we analyzed the uptake of iodinated EGF in control and in clathrin siRNA-treated cells. We observed only minor differences in the uptake rate (Fig. 9*C*).

When we analyzed the internalization of fluorescently labeled EGF upon α-adaptin depletion, we detected no significant difference to control cells. This suggests that a functional AP-2 adaptor is not required for the internalization of EGF (Fig. 8, *D* and *D′*). Since AP-2 expression is already strongly inhibited after 24 h, we also checked the uptake of EGF on day 1 after transfection and observed no significant inhibition (Fig. 8, *E* and *E′*). This observation suggests that the lack of inhibition is not due to a slow up-regulation of an alternative uptake mechanism for EGF.

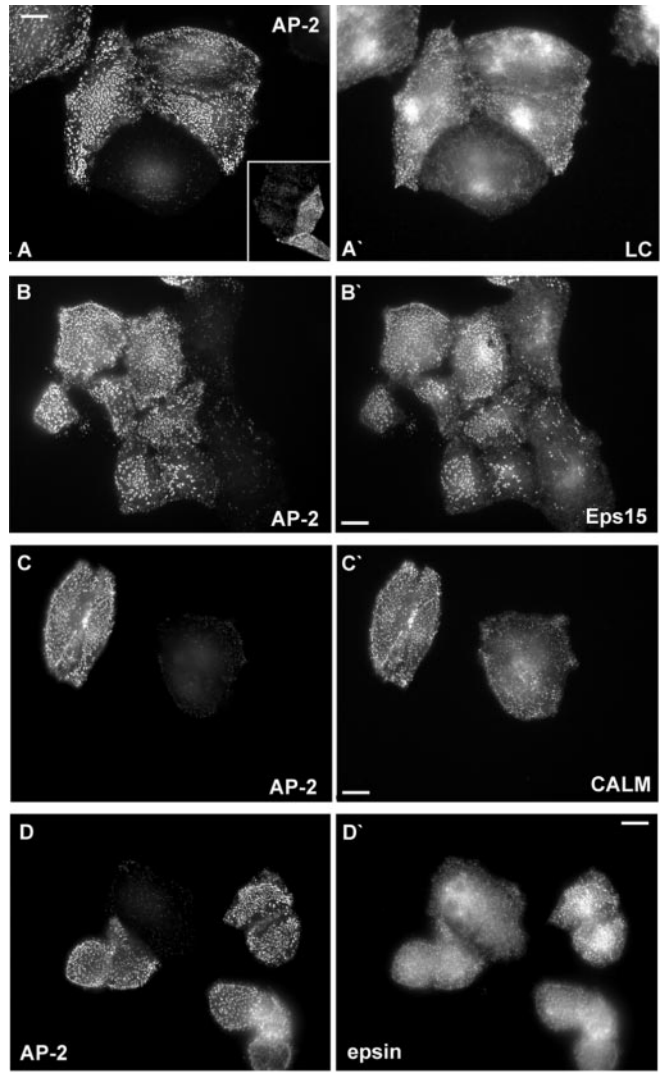

FIG. 6. **The effect of α-adaptin depletion on clathrin and the accessory proteins CALM, Eps15, and epsin.** HeLa cells transfected with α-adaptin siRNA oligo I were mixed with control cells 24 h after transfection and cocultivated for another 24 h. The cells were then double stained for α-adaptin (*A–D*) and LC (*A′*), Eps15 (*B′*), CALM (*C′*), and epsin (*D′*). Note that the plasma membrane association of clathrin LC and Eps15 were strongly reduced. A subtle effect on CALM was also observed. *Inset* in *A*, transfection with α-adaptin-specific siRNA oligo II. The *bar* corresponds to 10 μm.

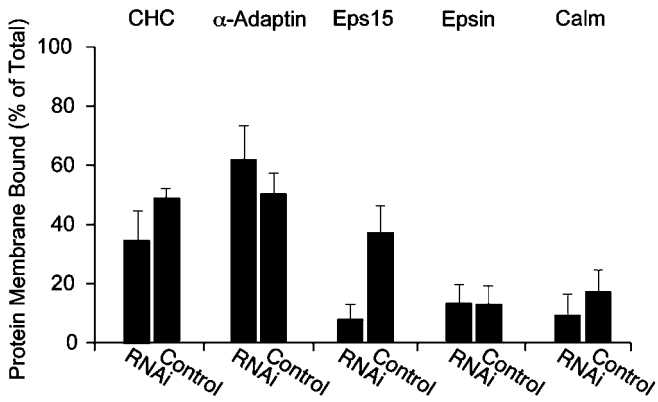

FIG. 7. **Membrane association of coat proteins upon α-adaptin depletion.** α-Adaptin siRNA-transfected and mock-transfected cells were scraped in lyses buffer and then fractionated by ultracentrifugation into a membrane and a cytosol pool. The fractions were subjected to SDS-PAGE and visualized by Western blotting using enhanced chemiluminescence. The signals were quantitated by densitometry. Note that only the clathrin heavy chains and especially Eps15 were released to a significant extent into the cytosolic pool, whereas residual α-adaptin in the knockdown cells was predominantly membrane-associated.

Taken together our data show that clathrin and AP-2 are absolutely required for efficient transferrin uptake. In the case of EGF, clathrin seems not essential for the uptake but seems to be required for accumulation of internalized EGF in multivesicular endosomes. This might explain why the knockdown of α-adaptin, which functions mainly in initial steps in endocytosis, had little effect on EGF uptake.

DISCUSSION

To analyze the contributions of individual endocytic proteins to the formation of clathrin-coated vesicles, we used RNAi to deplete the clathrin heavy chain and the α subunit of the AP-2 adaptor in HeLa cells. As judged by semiquantitative Western blotting, transfection with heavy chain-specific siRNA reduced the cellular clathrin concentration to less than ten percent within 3 days. The estimated half-life of clathrin in transfected HeLa cells corresponded to only 18–20 h. This is consistent with the half-life of clathrin in DT40 lymphocytes where the heavy chain gene was replaced by a clathrin cDNA under the control of a tetracycline-regulatable promoter (52). In contrast, a half-life of ~50 h for the clathrin heavy chain was determined by pulse-chase experiments in the mouse B cell lymphoma line (53). At this point we do not know whether a sudden interference with clathrin expression might indirectly shorten its life span or whether the half-life of clathrin is a function of cell type and/or species. Concomitantly with the depletion of the heavy chain we noted a reduction in cellular light chain concentration, indicating that free light chains are not stable in cytosol. Clathrin depletion had, however, little effect on the intracellular concentrations of adaptors, epsin, Eps15, and CALM. Very recently it was reported that upon expression of clathrin antisense RNA in baby hamster kidney cells the steady-state level of dynamin increased 10-fold within 2 days of antisense RNA induction (64). Parallel to this increase in the level of dynamin an accumulation of clathrin-coated pits on the plasma membrane and on endosomes was noted. Most strikingly, however, was the observation that many of the coated pits were connected to the plasma membrane by long dynamin-wrapped tubules. Moreover, a very early inhibition of transferrin uptake took already effect when the clathrin concentration was reduced by only 10% (64). Although we also noted a clathrin RNAi-induced relative increase in shallow coated pits at the expense of deeply invaginated and/or coated vesicles, long dynamin-wrapped tubules were never observed, even when serial sections were examined (data not shown). We also did not detect an increase in the level of dynamin upon clathrin depletion (Fig. 3*C*). These apparent discrepancies between our observations and that of Iversen *et al*. (64) might be explained by different experimental approaches and/or the use of different cell lines.

The accumulation of shallow pits after clathrin depletion in HeLa is consistent with recent observation in living cells. FRAP (fluorescence recovery after photo bleaching) measurements indicated that clathrin triskelia rapidly exchange between the cytosolic pool and membrane-associated lattices (66). It was suggested that this exchange might underlie the reorganization of the clathrin lattice during the budding process (66). In this scenario a limiting supply of cytosolic clathrin protomers might then be expected to slow this exchange, resulting in an accumulation of shallow coated pits. This interpretation is also supported by the results of our cell fractionation studies, which indicated that the residual clathrin of knockdown cells was preferentially membrane-associated. This observation could also explain a discrepancy that was noted when the effects of the clathrin knockdown were analyzed by semiquantitative Western blotting and by ultrastructural analysis. Whereas 2 days after transfection the former indicated a depletion of the clathrin heavy chain by ~80%, coated membranes appeared to be reduced by only 60%.

Depletion of clathrin had only a small effect on the membrane association of AP-1, AP-2, and CALM and not a significant one on epsin and dynamin. Only the fluorescence signal of Eps15 appeared consistently stronger in clathrin-depleted cells. However, we do not think that this reflects an increase in the membrane association of Eps15 when clathrin is depleted, because Western blots of the membrane fraction did not suggest a shift from the cytosolic pool of Eps15 to the membrane fraction. More likely is an increased accessibility of Eps15 for antibodies when clathrin is not present. Despite the induced strong reduction of the clathrin level, all endocytic proteins that were investigated here retained their punctate staining pattern, which suggests that they are still concentrated on the membrane in patches. Similar observations were made previously with the adaptors AP-2 and AP-1. Overexpression of auxilin 2 (cyclin G-associated kinase) caused clathrin to aggregate together with auxilin 2 into large perinuclear aggresomes, whereas the punctate distribution of AP-2 remained unaltered (39). AP-1 staining was also not affected in these cells. Eisenberg and co-workers (68) made similar observations when they overexpressed auxilin or AP180. Clathrin-independent membrane association of adaptors was also confirmed when clathrin was repressed in DT-40 lymphocytes (52) and in engineered BHK21 cells that expressed antisense clathrin heavy chain (64).

Clathrin depletion caused a change in the localization of EEA1- and Hrs-positive endosomal structures to the perinuclear area. Similarly we noted a relocation of the large mannose 6-phosphate receptor to this region. These observations are consistent with results obtained by overexpressing clathrin fragments that lack N-terminal and distal domains in HeLa cells, which demonstrated a similar redistribution of the endosomal compartment (60).

Depletion of α-adaptin from HeLa cells occurred not only very efficiently but also unusually rapid. Within 24 h more than 90% of the α-adaptin signal was gone indicating a very high turnover rate for this protein. The knockdown had also a profound effect on the membrane association of clathrin and Eps15. By electron microscopy we only very rarely detected peripheral clathrin coats, whereas numerous coated structures were still present in the Golgi region (data not shown). This

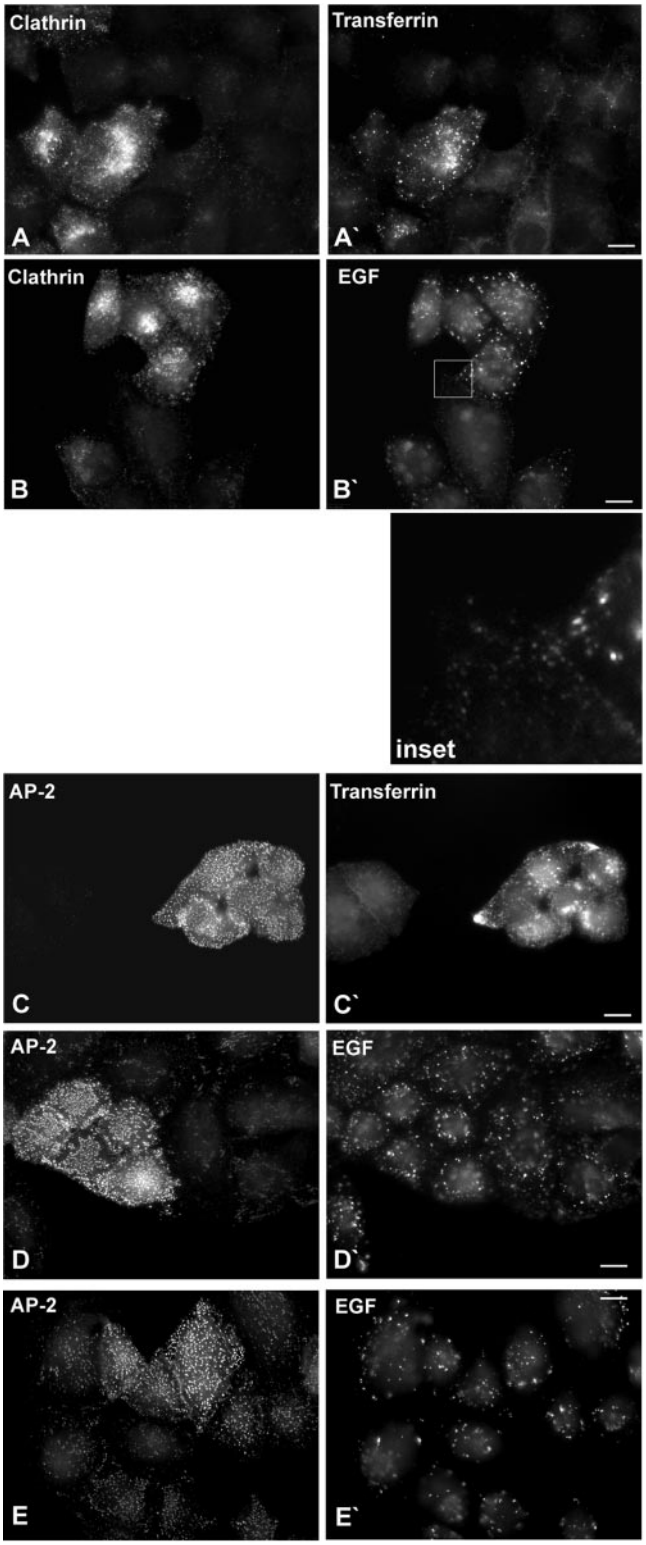

FIG. 8. **Uptake of transferrin and EGF upon clathrin heavy chain and α-adaptin depletion.** 48 h post-transfection serum-starved siRNA-transfected HeLa cells were incubated with fluorescence-labeled transferrin or EGF for 1 h on ice followed by a wash and an incubation with serum free medium for 10 min at 37 °C. The cells were then fixed and stained for AP-2 or clathrin heavy chain. *A* and *A′*, transferrin uptake after transfection with clathrin siRNA; *B* and *B′*, EGF uptake after transfection with clathrin siRNA; *C* and *C′*, transferrin uptake after transfection with α-adaptin siRNA; *D* and *D′*, EGF uptake after transfection with α-adaptin siRNA; *E* and *E′*, EGF uptake after transfection with α-adaptin siRNA 24 h after transfection with α-adaptin-specific siRNA. Note that transfection with α-adaptin-specific siRNA strongly affected the uptake of transferrin, whereas that of EGF appeared to be normal. *Bar* corresponds to 10 μm.

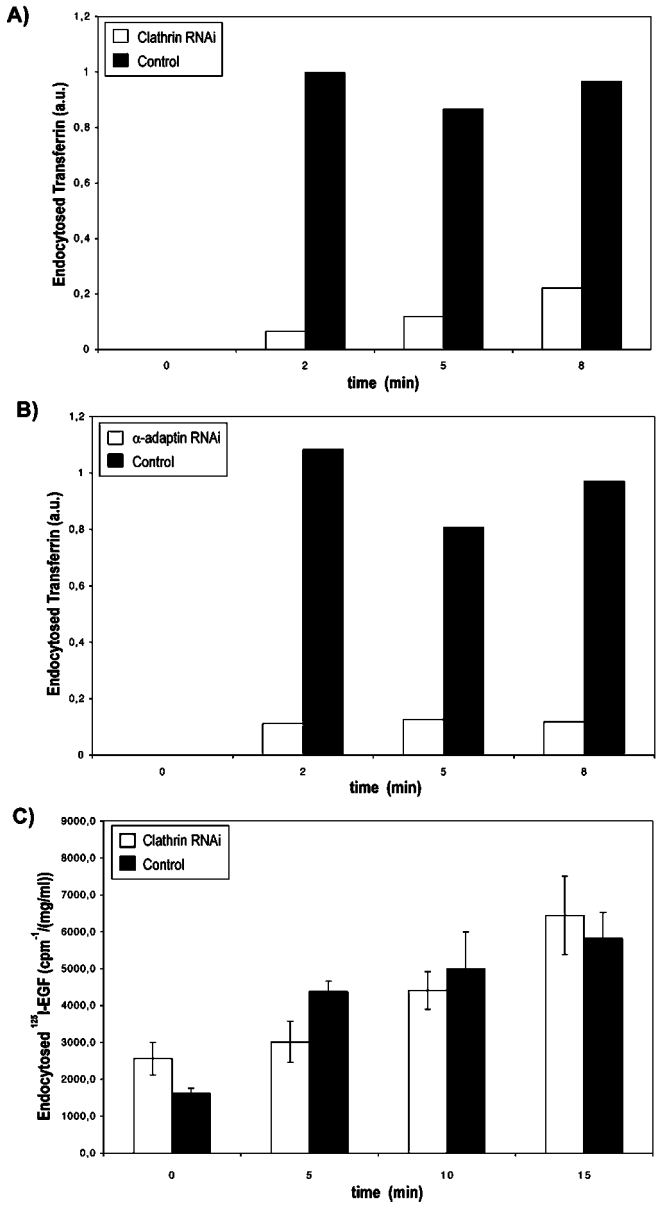

FIG. 9. **Quantitation of transferrin and EGF endocytosis upon clathrin heavy chain and α-adaptin depletion.** *A*, 48 h post-transfection clathrin siRNA-transfected and mock-transfected HeLa cells were serum-starved and then incubated with biotin-labeled transferrin for 1 h on ice followed by an incubation at 37 °C for the indicated times. The cells were acid washed and then analyzed by Western blotting. Peroxidase-conjugated NeutrAvidin was used to quantify the uptake. The intensity is shown in arbitrary units (*a.u.*). *B*, the same procedure as described in the legend to A was used for HeLa cells transfected with α-adaptin-specific siRNA. *C*, serum-starved transfected and non transfected HeLa cells depleted of the clathrin heavy chain were incubated with ^{125}I-labeled EGF for 1 h on ice followed by an incubation at 37 °C for the indicated times. The cells were then acid-washed, and the radioactivity was determined in a γ-counter. *Bars* are averages of three independent measurements. Note that clathrin depletion had little effect on the uptake of EGF.

result clearly demonstrated the importance of AP-2 for the stable membrane association of both proteins. For clathrin this was expected, but not necessarily for Eps15. This protein was considered to be essential for the recruitment of AP-2 to the plasma membrane, because a mutant Eps15 that lacked two of its three EH domains failed to localize to membranes and moreover prevented the membrane association of AP-2 and clathrin (23). In a different experimental setting, permeabilized HER14 fibroblasts, stably transfected with EGF receptor,

were extracted with 0.5 M Tris and then analyzed by immunofluorescence for the presence of Eps15. Whereas clathrin and AP-2 were completely extracted by Tris, Eps15 still retained a punctate staining distribution suggesting an association with the membrane that is independent of AP-2 and clathrin (69). These observations strongly supported a function for Eps15 in recruiting AP-2 to the plasma membrane. However, our results described here show that Eps15 also requires AP-2 for its localization to the membrane and suggest that only a complex of AP-2 and Eps15 has membrane binding competence. Once properly bound, Eps15 might resist extraction by Tris *in vitro* better than other coat components, but this does not necessarily reflect the order of recruitment to the membrane *in vivo*.

The extent of the membrane association of the accessory protein CALM was also reduced after depletion of α-adaptin. This effect is probably directly linked to the depletion of AP-2 rather than that of clathrin, since depletion of clathrin did not effect membrane association of CALM significantly. In contrast epsin seemed to interact normally with the plasma membrane in the absence of AP-2 and clathrin, possibly by virtue of its affinity for the membrane lipid PIP_2 (8).

To examine the functional consequences of the clathrin and α-adaptin depletions, we tested the uptake of transferrin and EGF. Transferrin uptake was blocked upon clathrin and AP-2 depletion. This result was not unexpected, since it is well established that the transferrin receptor enters cells through clathrin-coated pits (70). In contrast EGF uptake by HeLa cells was not significantly affected by clathrin depletion as indicated by the uptake of radiolabeled EGF. However, the intracellular trafficking of EGF differed from that in control cells where we observed fluorescently labeled EGF within 10 min in large EEA1- and Hrs-positive structures, which are likely to correspond to MVE. It is believed that activated signaling receptors are sorted into the membrane of the luminal vesicles for degradation by lysosomal enzymes. However, after clathrin depletion, the EGF did not accumulate in Hrs-positive structures but remained finely dispersed in small vesicular structures that are not accessible from the cell surface. In contrast α-adaptin depletion did not prevent the accumulation of EGF in Hrs-positive organelles. Taken together, our data suggest that in HeLa cells the internalization of EGF does not depend on the clathrin, but it is essential for EGF sorting to MVE. A flat bilayered clathrin coat found on the limiting membrane of MVE has been implicated recently in the sorting of ubiquitinated receptors into the internal vesicles (61). Thus, it is likely that clathrin depletion interferes with this process.

Although a number of previous reports have stressed an involvement of AP-2 in the uptake of EGF (65, 69, 71–73), there are at least three reports that are consistent with our observations. EGFR mutants that lack the AP-2 binding determinant were down-regulated in B82 fibroblasts with similar kinetics as the wild type receptor (74). Moreover, it has been shown that a dominant negative μ_2 subunit of AP-2 impairs the uptake of transferrin but not that of EGF (75). Very recently it was shown that overexpression of a C-terminal fragment of AP180, which efficiently blocks transferrin uptake, did not interfere with the EGF-induced uptake of EGFR (76). More, albeit indirect, evidence for an alternative entry route of EGF into HeLa cells came from observations we made with β-methylcyclodextrin. This reagent extracts cholesterol from membranes and is known to inhibit the budding of clathrin coated pits. This leads to an accumulation of shallow coated pits (77). Whereas transferrin was readily concentrated within these structures, we noted only rarely colocalization of EGF with these pits (data not shown). What might be an alternative uptake mechanism for EGF? There is already convincing evidence that the activated EGFR induces membrane ruffles that result in the formation of macropinocytic structures (59, 67, 76). Macropinocytosis involves primarily the actin-based cytoskeleton rather than the clathrin endocytosis machinery, and it is therefore unlikely to be affected by a clathrin knockdown. We therefore think that in HeLa cells EGF uptake via clathrin-coated pits plays only a very minor role but clathrin is essential for its accumulation in EEA1- and Hrs-positive organelles.

To confirm the specificity of the clathrin heavy chain siRNA, we transfected HeLa cells with a second RNA duplex (HC oligo II), which targeted a different sequence within the open reading frame of the heavy chain gene. HC oligo II silenced the expression of the heavy chain to a similar extent. In contrast when HC oligo I was transfected into mouse fibroblasts no silencing was obtained, because the target sequence differs in three positions. Similarly, a second α-adaptin-specific RNA duplex was effective in silencing the expression of α-adaptin in Hela cells, and as predicted on the basis of conserved target sequences in man and mouse, the α-oligo I silenced α-adaptin in both species.

Although clathrin depletion clearly diminished the growth rate of HeLa cells, they were nevertheless capable of adjusting to the depletion of at least 80% of their endogenous clathrin without undergoing apoptosis. Moreover, under optimal growth conditions they readily coped with the depletion of more than 95% of their endogeneous α-adaptin without dying. This adaptive potential of the HeLa cells will allow a systematic dissection of the function of individual endocytic proteins by RNAi, but it will also require more sophisticated phenotype analysis such as internalization kinetics and observations of the coated pit dynamics in living cells.

Acknowledgments—We thank B. Grossmann, C. Lemke, and E. Mallon for expert technical assistance; A. Hundt for photographic work; B. Hoflack, L. Traub, H. Stenmark, and M. Zerial for supplying essential reagents; and R. Bauerfeind and A. Ungewickell for helpful comments on the manuscript.

REFERENCES

1. Brodsky, F. M., Chen, C. Y., Knuehl, C., Towler, M. C., and Wakeham, D. E. (2001) *Annu. Rev. Cell Dev. Biol.* **17,** 517–568
2. van Dam, E. M., and Stoorvogel, W. (2002) *Mol. Biol. Cell* **13,** 169–182
3. Stahl, P. D., and Barbieri, M. A. (2002) *Science's STKE* http:/stke.sciencemag.org/cgi/content/full/OC_sigtrans;2002/141/pe32
4. Katzmann, D. J., Babst, M., and Emr, S. D. (2001) *Cell* **106,** 145–155
5. Stoorvogel, W., Oorschot, V., and Geuze, H. J. (1996) *J. Cell Biol.* **132,** 21–33
6. Sachse, M., Urbe, S., Oorschot, V., Strous, G. J., and Klumperman, J. (2002) *Mol. Biol. Cell* **13,** 1313–1328
7. Raiborg, C., Bache, K. G., Mehlum, A., Stang, E., and Stenmark, H. (2001) *EMBO J.* **20,** 5008–5021
8. Ford, M. G., Pearse, B. M., Higgins, M. K., Vallis, Y., Owen, D. J., Gibson, A., Hopkins, C. R., Evans, P. R., and McMahon, H. T. (2001) *Science* **291,** 1051–1055
9. Takei, K., and Haucke, V. (2001) *Trends Cell Biol.* **11,** 385–391
10. Stahelin, R. V., Long, F., Peter, B. J., Murray, D., De Camilli, P., McMahon, H. T., and Cho, W. (2003) *J. Biol. Chem.* **278,** 28993–28999
11. Chen, H., Fre, S., Slepnev, V. I., Capua, M. R., Takei, K., Butler, M. H., Di Fiore, P. P., and De Camilli, P. (1998) *Nature* **394,** 793–797
12. Rosenthal, J. A., Chen, H., Slepnev, V. I., Pellegrini, L., Salcini, A. E., Di Fiore, P. P., and De Camilli, P. (1999) *J. Biol. Chem.* **274,** 33959–33965
13. Owen, D. J., Vallis, Y., Noble, M. E., Hunter, J. B., Dafforn, T. R., Evans, P. R., and McMahon, H. T. (1999) *Cell* **97,** 805–815
14. Owen, D. J., Vallis, Y., Pearse, B. M., McMahon, H. T., and Evans, P. R. (2000) *EMBO J.* **19,** 4216–4227
15. Ahle, S., and Ungewickell, E. (1986) *EMBO J.* **5,** 3143–3149
16. Morgan, J. R., Prasad, K., Hao, W., Augustine, G. J., and Lafer, E. M. (2000) *J. Neurosci.* **20,** 8667–8676
17. Drake, M. T., Downs, M. A., and Traub, L. M. (2000) *J. Biol. Chem.* **275,** 6479–6489
18. Drake, M. T., and Traub, L. M. (2001) *J. Biol. Chem.* **276,** 28700–28709
19. Dell'Angelica, E. C. (2001) *Trends Cell Biol.* **11,** 315–318
20. Tebar, F., Bohlander, S. K., and Sorkin, A. (1999) *Mol. Biol. Cell* **10,** 2687–2702
21. Kalthoff, C., Alves, J., Urbanke, C., Knorr, R., and Ungewickell, E. J. (2001) *J. Biol. Chem.* **277,** 8209–8216
22. Benmerah, A., Begue, B., Dautry-Varsat, A., and Cerf-Bensussan, N. (1996) *J. Biol. Chem.* **271,** 12111–12116
23. Benmerah, A., Bayrou, M., Cerf-Bensussan, N., and Dautry-Varsat, A. (1999) *J. Cell Sci.* **112,** 1303–1311
24. Tebar, F., Sorkina, T., Sorkin, A., Ericsson, M., and Kirchhausen, T. (1996) *J. Biol. Chem.* **271,** 28727–28730

25. Torrisi, M. R., Lotti, L. V., Belleudi, F., Gradini, R., Salcini, A. E., Confalonieri, S., Pelicci, P. G., and Di Fiore, P. P. (1999) *Mol. Biol. Cell* **10,** 417–434
26. Bache, K. G., Raiborg, C., Mehlum, A., and Stenmark, H. (2003) *J. Biol. Chem.* **278,** 12513–12521
27. Bean, A. J., Davanger, S., Chou, M. F., Gerhardt, B., Tsujimoto, S., and Chang, Y. (2000) *J. Biol. Chem.* **275,** 15271–15278
28. Benmerah, A., Lamaze, C., Begue, B., Schmid, S. L., Dautry-Varsat, A., and Cerf-Bensussan, N. (1998) *J. Cell Biol.* **140,** 1055–1062
29. Miller, W. E., and Lefkowitz, R. J. (2001) *Curr. Opin. Cell Biol.* **13,** 139–145
30. Goodman, O. B., Jr., Krupnick, J. G., Santini, F., Gurevich, V. V., Penn, R. B., Gagnon, A. W., Keen, J. H., and Benovic, J. L. (1996) *Nature* **383,** 447–450
31. Morris, S. M., and Cooper, J. A. (2001) *Traffic* **2,** 111–123
32. Mishra, S. K., Keyel, P. A., Hawryluk, M. J., Agostinelli, N. R., Watkins, S. C., and Traub, L. M. (2002) *EMBO J.* **21,** 4915–4926
33. Shupliakov, O., Low, P., Grabs, D., Gad, H., Chen, H., David, C., Takei, K., De Camilli, P., and Brodin, L. (1997) *Science* **276,** 259–263
34. Vallee, R. B., Herskovits, J. S., Aghajanian, J. G., Burgess, C. C., and Shpetner, H. S. (1993) *CIBA Found Symp* **176,** 185–193; 193–187
35. van der Bliek, A. M., Redelmeier, T. E., Damke, H., Tisdale, E. J., Meyerowitz, E. M., and Schmid, S. L. (1993) *J. Cell Biol.* **122,** 553–563
36. Herskovits, J. S., Burgess, C. C., Obar, R. A., and Vallee, R. B. (1993) *J. Cell Biol.* **122,** 565–578
37. Cremona, O., Di Paolo, G., Wenk, M. R., Luthi, A., Kim, W. T., Takei, K., Daniell, L., Nemoto, Y., Shears, S. B., Flavell, R. A., McCormick, D. A., and De Camilli, P. (1999) *Cell* **99,** 179–188
38. Ungewickell, E., Ungewickell, H., Holstein, S. E., Lindner, R., Prasad, K., Barouch, W., Martin, B., Greene, L. E., and Eisenberg, E. (1995) *Nature* **378,** 632–635
39. Umeda, A., Meyerholz, A., and Ungewickell, E. (2000) *Eur. J. Cell Biol.* **79,** 336–342
40. Newmyer, S. L., and Schmid, S. L. (2001) *J. Cell Biol.* **152,** 607–620
41. Schlossman, D. M., Schmid, S. L., Braell, W. A., and Rothman, J. E. (1984) *J. Cell Biol.* **99,** 723–733
42. Greener, T., Zhao, X., Nojima, H., Eisenberg, E., and Greene, L. E. (2000) *J. Biol. Chem.* **275,** 1365–1370
43. Qualmann, B., and Kessels, M. M. (2002) *Int. Rev. Cytol.* **220,** 93–144
44. Elbashir, S. M., Harborth, J., Lendeckel, W., Yalcin, A., Weber, K., and Tuschl, T. (2001) *Nature* **411,** 494–498
45. Chin, D. J., Straubinger, R. M., Acton, S., Nathke, I., and Brodsky, F. M. (1989) *Proc. Natl. Acad. Sci. U. S. A.* **86,** 9289–9293
46. Brodsky, F. M. (1985) *J. Cell Biol.* **101,** 2055–2062
47. Ahle, S., Mann, A., Eichelsbacher, U., and Ungewickell, E. (1988) *EMBO J.* **7,** 919–929
48. Harborth, J., Elbashir, S. M., Bechert, K., Tuschl, T., and Weber, K. (2001) *J. Cell Sci.* **114,** 4557–4565
49. Lindner, R., and Ungewickell, E. (1992) *J. Biol. Chem.* **267,** 16567–16573
50. Sorkin, A., and Carpenter, G. (1991) *J. Biol. Chem.* **266,** 23453–23460
51. Leers, M. P., Kolgen, W., Bjorklund, V., Bergman, T., Tribbick, G., Persson, B., Bjorklund, P., Ramaekers, F. C., Bjorklund, B., Nap, M., Jornvall, H., and Schutte, B. (1999) *J. Pathol.* **187,** 567–572
52. Wettey, F. R., Hawkins, S. F., Stewart, A., Luzio, J. P., Howard, J. C., and Jackson, A. P. (2002) *Science* **297,** 1521–1525
53. Acton, S. L., and Brodsky, F. M. (1990) *J. Cell Biol.* **111,** 1419–1426
54. Sharp, P. A. (2001) *Genes Dev.* **15,** 485–490
55. Katzmann, D. J., Odorizzi, G., and Emr, S. D. (2002) *Nat. Rev. Mol. Cell. Biol.* **3,** 893–905
56. De Camilli, P., Chen, H., Hyman, J., Panepucci, E., Bateman, A., and Brunger, A. T. (2002) *FEBS Lett.* **513,** 11–18
57. Itoh, T., Koshiba, S., Kigawa, T., Kikuchi, A., Yokoyama, S., and Takenawa, T. (2001) *Science* **291,** 1047–1051
58. Meyer, C., Zizioli, D., Lausmann, S., Eskelinen, E. L., Hamann, J., Saftig, P., von Figura, K., and Schu, P. (2000) *EMBO J.* **19,** 2193–2203
59. Lynch, D. K., Winata, S. C., Lyons, R. J., Hughes, W. E., Lehrbach, G. M., Wasinger, V., Corthals, G., Cordwell, S., and Daly, R. J. (2003) *J. Biol. Chem.* **278,** 21805–21813
60. Bennett, E. M., Lin, S. X., Towler, M. C., Maxfield, F. R., and Brodsky, F. M. (2001) *Mol. Biol. Cell* **12,** 2790–2799
61. Raiborg, C., Bache, K. G., Gillooly, D. J., Madshus, I. H., Stang, E., and Stenmark, H. (2002) *Nat. Cell Biol.* **4,** 394–398
62. Raiborg, C., Bremnes, B., Mehlum, A., Gillooly, D. J., D'Arrigo, A., Stang, E., and Stenmark, H. (2001) *J. Cell Sci.* **114,** 2255–2263
63. Pearse, B. M. (1976) *Proc. Natl. Acad. Sci. U. S. A.* **73,** 1255–1259
64. Iversen, T. G., Skretting, G., Van Deurs, B., and Sandvig, K. (2003) *Proc. Natl. Acad. Sci. U. S. A.* **100,** 5175–5180
65. Benmerah, A., Gagnon, J., Begue, B., Megarbane, B., Dautry-Varsat, A., and Cerf-Bensussan, N. (1995) *J. Cell Biol.* **131,** 1831–1838
66. Wu, X., Zhao, X., Baylor, L., Kaushal, S., Eisenberg, E., and Greene, L. E. (2001) *J. Cell Biol.* **155,** 291–300
67. Bretscher, M. S., and Aguado-Velasco, C. (1998) *Curr. Biol.* **8,** 721–724
68. Zhao, X., Greener, T., Al-Hasani, H., Cushman, S. W., Eisenberg, E., and Greene, L. E. (2001) *J. Cell Sci.* **114,** 353–365
69. van Delft, S., Schumacher, C., Hage, W., Verkleij, A. J., and van Bergen en Henegouwen, P. M. (1997) *J. Cell Biol.* **136,** 811–821
70. Hanover, J. A., Willingham, M. C., and Pastan, I. (1984) *Cell* **39,** 283–293
71. Nesterov, A., Kurten, R. C., and Gill, G. N. (1995) *J. Biol. Chem.* **270,** 6320–6327
72. Sorkin, A., McKinsey, T., Shih, W., Kirchhausen, T., and Carpenter, G. (1995) *J. Biol. Chem.* **270,** 619–625
73. Boll, W., Gallusser, A., and Kirchhausen, T. (1995) *Curr. Biol.* **5,** 1168–1178
74. Nesterov, A., Wiley, H. S., and Gill, G. N. (1995) *Proc. Natl. Acad. Sci. U. S. A.* **92,** 8719–8723
75. Nesterov, A., Carter, R. E., Sorkina, T., Gill, G. N., and Sorkin, A. (1999) *EMBO J.* **18,** 2489–2499
76. Yamazaki, T., Zaal, K., Hailey, D., Presley, J., Lippincott-Schwartz, J., and Samelson, L. E. (2002) *J. Cell Sci.* **115,** 1791–1802
77. Subtil, A., Gaidarov, I., Kobylarz, K., Lampson, M. A., Keen, J. H., and McGraw, T. E. (1999) *Proc. Natl. Acad. Sci. U. S. A.* **96,** 6775–6780

Membrane Transport, Structure, Function, and Biogenesis:

Effect of Clathrin Heavy Chain- and α -Adaptin-specific Small Inhibitory RNAs on Endocytic Accessory Proteins and Receptor Trafficking in HeLa Cells

Lars Hinrichsen, Jens Harborth, Lars Andrees, Klaus Weber and Ernst J. Ungewickell

J. Biol. Chem. 2003, 278:45160-45170.
doi: 10.1074/jbc.M307290200 originally published online September 6, 2003